ChemComm

Check for updates

Dioxygen splitting at room temperature over distant binuclear transition metal centers in zeolites for direct oxidation of methane to methanol†

Kinga Mlekodaj, [ID] [a] Mariia Lemishka,[ab] Stepan Sklenak, [ID] [a] Jiri Dedecek[a] and Edyta Tabor [ID] *[a]

Here we demonstrate for the first time the splitting of dioxygen at RT over distant binuclear transition metal (M = Ni, Mn, and Co) centers stabilized in ferrierite zeolite. Cleaved dioxygen directly oxidized methane to methanol, which can be released without the aid of an effluent to the gas phase at RT.

Employment of dioxygen as an abundant, eco-friendly, and low-cost oxidant represents one of the greatest challenges in oxidation catalysis.[1–5] Nature activates dioxygen over transition metal cations inside enzymes for a direct oxidation, *e.g.*, methane to methanol.[4,6] From an industrial point of view, the direct transformation of methane, representing the dominant component of natural and shale gases, into methanol is enormously requested. Instead of the highly energy demanding and costly methane steam reforming with breaking the C–H bond to yield syngas $(CO + H_2)$ followed by reformation of the C–H bond into hydrocarbons (Fischer–Tropsch synthesis), a direct route of oxidation of methane to methanol would be a dramatic step ahead in methane processing. Nevertheless, the latter is economically feasible only when using a cheap oxidant such as dioxygen. The first selective oxidation of methane at 100–200 °C by dioxygen over synthetic catalysts was reported for Cu-ZSM-5 and Cu-mordenite zeolites.[2,7–10] However, the activation of dioxygen over these zeolites required high temperatures of 180–450 °C, the yields of methanol were low (4–140 μmol g^{-1}), and moreover, the produced methanol had to be extracted from the catalyst by water. Di-copper, tri-copper, and larger (Cu$_n$, $n > 3$) Cu-oxo species were suggested as the active sites.[3,7–9,11–13] However, the yields of methanol produced from methane using dioxygen were unsatisfactory both in the stoichiometric and catalytic regimes.[2,6]

Transition metal cations stabilized in extra-framework cationic sites in zeolite can be considered as inorganic analogues of active sites in metalloenzymes due to their open coordination sphere and ability to maintain redox cycling.[4,6] Very recently, a break-through in dioxygen activation over Fe-zeolites of the ferrierite topology (FER) was achieved.[4] Two cooperating distant Fe cations in Fe-ferrierite carrying a four electron process of dioxygen dissociation undergo an M(II) → M(IV) redox cycle similarly to redox processes occurring over Fe active sites in methane monooxygenase.[6] The distant binuclear cationic Fe(II) centers in Fe-ferrierite are close enough to cooperate in splitting dioxygen at RT resulting in the formation of a pair of active oxygen species called the α-oxygen.[4,14–16] However, the distance between cations in Fe-ferrierite is significantly larger (7.4 Å) than those reported for metalloenzymes (< 4 Å), and thus the dioxygen activation over Fe-ferrierite results in a dioxygen dissociation into a pair of distant α-oxygens instead of the formation of bis(μ-oxo)diiron or (μ-peroxo)diiron bridges created in metalloenzymes.[3,4] DFT calcu-lated barriers of splitting dioxygen (25 kcal mol^{-1}) over Fe-ferrierite reveal facile oxidation of Fe(II) cations of Fe-ferrierite, which can be explained by the unique topology of the ferrierite zeolite.[4,16] To form the active Fe(II) sites, specific Al distribution in the ferrierite matrix is required. Al atoms in the ferrierite framework are organized as a pair of negatively charged Al atoms in 6-rings (*i.e.*, Al–O–Si–O–Si–O–Al sequence, Fig. 1A), which is strictly required for balancing a bare divalent cation (Fig. 1B), forming further a distant binuclear cationic structure located across the ferrierite channel (Fig. 1C).[4,16] The organization of Al atoms in zeolite frameworks induces the explicit geometry and position for cationic sites in the zeolitic matrix, which can be occupied by divalent transition metal ions. In the case of ferrierite, three cationic sites α, β, and γ can be distinguished.[4,16,17] However, only the cations located in the β sites can form the distant binuclear cationic centers (Fig. 1C).

It was shown that binuclear Fe centers in ferrierite already at Fe/Al 0.04 are able to utilize dioxygen to form a pair of α-oxygens (Fig. 1D), used further for direct methane to methanol oxidation. This raises a question of whether the ability to cleave

*[a] J. Heyrovský Institute of Physical Chemistry of the CAS, v. v. i,
Dolejškova 2155/3, Prague 182 23, Czech Republic
E-mail: edyta.tabor@jh-inst.cas.cz
[b] University of Pardubice, Studentská 95, Pardubice 532 10, Czech Republic*
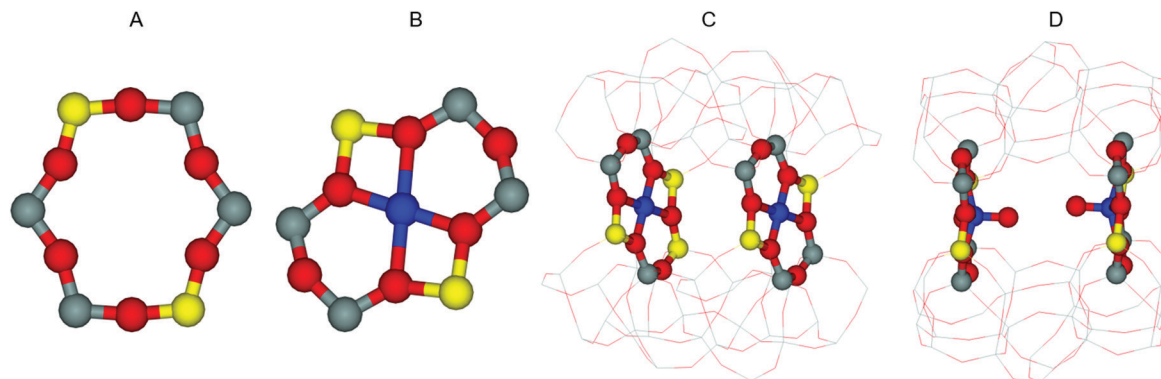
Fig. 1 Schematic representation of distant binuclear cationic sites in ferrierite. (A) The arrangement of the Al pair (Al−O−Si−O−Si−O−Al sequence) in the 6-ring of the β site. (B) The coordination of a bare divalent cation in the β site. (C) The arrangement of distant binuclear cationic centers. (D) A pair of distant α-oxygens originating from splitting O_2 over distant binuclear cationic structures.

dioxygen is a general feature of distant binuclear transition metal cations.

In this contribution, we explore the previously theoretically predicted[4,18] general ability of transition metal ions (Ni, Mn, Co) in binuclear centers in ferrierite to dissociate dioxygen at RT to give a pair of distant α-oxygens. The exceptional oxidation properties of a pair of α-oxygens is further tested in direct oxidation of methane to methanol already at RT. The application of Ni, Mn, and Co cations instead of Fe-exchanged ferrierite eliminats major drawback of iron containing zeolites connected with transformation of Fe(II) species under oxidation reaction conditions into inactive Fe(III) oxo-ones.[19] Furthermore, preparation of Fe-zeolites represents a time consuming and multistep process involving removal of organic medium,[19,20] while the introduction of Ni, Mn, and Co to

ferrierite can be performed by simple methods such as ion-exchange from the solution or impregnation from an inorganic source.[16,17] Such an improvement in preparation and stability of cationic active centers makes systems based on Ni, Mn, or Co-ferrierite attractive for employment as potential catalysts in methane to methanol oxidation on the industrial level. Moreover, in contrast to previously studied zeolitic systems for methane to methanol oxidation, Fe-ferrierite with a high population of binuclear Fe(II) sites does not require usage of the effluent to protonate the methoxy species and to extract the oxidation product from the catalyst. This is a huge step ahead in methanol production, and represents the next advantage of the proposed redox system.

Previously performed Al distribution in H-ferrierite with Si/Al 8.6 revealed that 50% of Al atoms form Al pairs[21] (*i.e.*, Al−O−Si−O−Si−O−Al sequences, Fig. 1A) in the β cationic sites
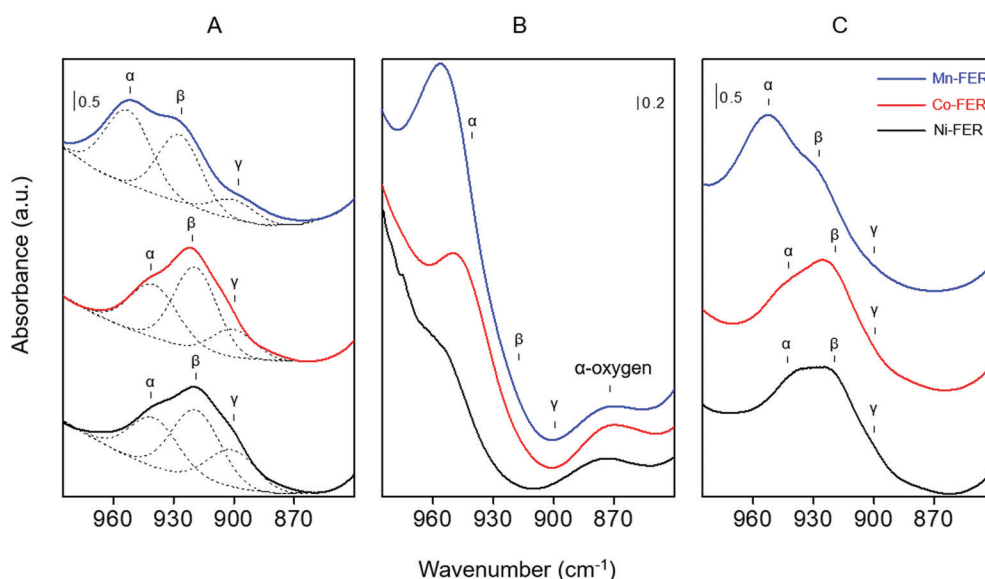

Fig. 2 FTIR spectra of Ni-, Mn-, and Co-ferrierite samples in the region of T−O−T vibrations recorded at RT after the following treatments: (A) an evacuation at 450 °C for 3 h, with the marked α, β, and γ cationic positions (dashed lines). (B) An evacuation at 450 °C for 3 h, followed by an interaction with O_2 (10^5 Pa) at RT for 1 h and subsequent desorption of O_2 at RT for 3 min. (C) An evacuation at 450 °C for 3 h, followed by an interaction with O_2 (10^5 Pa) at RT for 1 h and a subsequent desorption of O_2 at RT for 3 min, and a consecutive interaction with CH_4 (10^5 Pa) at RT for 1 h, and a desorption of CH_4 at 220 °C for 3 min.

(Fig. 1B),[18,19,22] which leads to highly populated binuclear M(II) sites (structural analysis of studied FER including Al distribution of Al atoms are presented in the ESI†).[22] This arrangement of Al atoms in the ferrierite framework guarantees at least 88% of the β sites participating in the formation of distant binuclear sites (Fig. 1C).[4,14,15] A set of three M-ferrierite (M = Ni, Mn, and Co) samples were prepared using an ion exchange for Co-ferrierite (Co/Al 0.18), and an impregnation procedure for Ni-ferrierite and Mn-ferrierite (Ni/Al 0.28 and Mn/Al 0.22).[17]

FTIR spectroscopy of the antisymmetric T–O–T stretching vibrations of the zeolite framework was used to investigate bare divalent cations accommodated in the individual cationic sites and their interaction with dioxygen.[4,16,22] FTIR spectra of the Ni-ferrierite, Mn-ferrierite, and Co-ferrierite evacuated at 450 °C exhibit a band in the range 1000–870 cm^{-1} which confirms the location of M(II) in the cationic sites (Fig. 2A). This band is not present in the FTIR spectrum of H-ferrierite (ESI,† Fig. S1). A deconvolution of this band revealed the three subspectra at around 940, 920, and 890 cm^{-1} assigned to the bare M(II) cations located in the α, β, and γ cationic sites, respectively (Fig. 2A).[4,16,17] The three M-ferrierite samples exhibited a high concentration of the M(II) cations in the β site (Table 1) which is essential for the formation of the distant binuclear centers.[4,16] The interaction of the evacuated M-ferrierite samples with dioxygen at RT resulted in the disappearance of the band attributed to the bare M(II) cations in the β cationic site followed by the formation of a new band at around 870 cm^{-1}. This band remains stable after the dioxygen desorption at RT (Fig. 2B). The vanishing of the band at 920 cm^{-1} characteristic for bare M(II) cations accommodated in the β site in M-ferrierite samples together with the simultaneous formation of the band at lower frequencies (870 cm^{-1}) due to stronger perturbation of the zeolite ring indicates that M(II) was oxidized by dioxygen to $[M(IV)=O]^{2+}$.[4,16] The band at around 870 cm^{-1} is a fingerprint of the α-oxygen formed from N_2O over Ni-, Co-, and Fe-ferrierite (ESI,† Fig. S2) and the α-oxygen created by dioxygen dissociation over Fe-ferrierite (ESI,† Fig. S3). This indicated that dioxygen was not only adsorbed at the distant binuclear Ni(II), Co(II), and Mn(II) centers in ferrierite but it was also cleaved at RT to form a pair of distant α-oxygen atoms analogously to the Fe-ferrierite.[4] Thus, these results provide the first evidence of splitting dioxygen and formation of the α-oxygen on non-iron distant binuclear sites in ferrierite at RT and the spectroscopic features of the α-oxygen originated from dioxygen dissociation were confirmed. These results unambiguously revealed that

splitting of dioxygen is a general feature of binuclear centers in M-ferrierite.

The α-oxygen is defined as the active oxygen form capable of oxidizing H_2, CO, benzene, and methane.[13,14] Therefore, the oxidation of these molecules represents unquestionable proof of the α-oxygen participation in the oxidation process. The oxidation of methane was selected as a model reaction for two main reasons. Firstly, methane is a very stable molecule with high bond dissociation energies (105 kcal mol^{-1}) requiring a highly reactive oxygen form to be oxidized. Secondly, there is enormous economic potential of the direct oxidation of methane to methanol, which is a strongly demanded transformation of natural gas to liquid products representing energy carriers and chemical production platforms.

The three M-ferrierite samples featuring pairs of the distant α-oxygen atoms originating from the oxidation by dioxygen at RT interact subsequently with methane at RT and are afterwards evacuated at 220 °C. The corresponding FTIR spectra are shown in Fig. 2C. This interaction leads to the disappearance of the band at 870 cm^{-1} and recovering the band at 920 cm^{-1} corresponding to the bare M(II) cations accommodated in the β cationic sites. The regeneration of the band at 920 cm^{-1} indicates that methane interacts with the α-oxygen atoms stabilized on M(II) in the β sites to form volatile products (Fig. 2C). Therefore, we conclude that our FTIR results evidence the formation of the α-oxygen atoms as the result of splitting dioxygen over distant binuclear Ni(II), Mn(II), and Co(II) cationic sites in M-ferrierites at RT. Furthermore, our results demonstrate that the products of the direct oxidation of methane by α-oxygen formed over the distant binuclear Ni(II), Mn(II), and Co(II) sites are easily released from the cationic centers.

Mass spectrometry was used for the detection of methanol resulting from the methane titration of the α-oxygens, previously formed by splitting dioxygen over distant binuclear Ni(II), Mn(II), and Co(II) centers in ferrierite. The M-ferrierite samples were activated at 450 °C, oxidized by dioxygen at RT, and subsequently, interacted with methane at RT. The mass spectrum revealed the presence of the signal with m/z = 31 (ESI,† Fig. S4) confirming the formation of methanol. These results proved that pairs of the α-oxygens from splitting dioxygen over all studied M-ferrierite samples are able to directly oxidize methane to methanol at RT. Moreover, methanol was detected in the stream of methane showing that it can be released at RT from the active M(II) sites and from a zeolite channel system to the gas stream without the need of an effluent. This feature of the studied distant binuclear centers in M-ferrierite represents a significant advantage in comparison with the other metallozeolite systems requiring application of an effluent for the release of the products of the selective oxidation of methane.[2,6,7]

The obtained yields of methanol (Table 1) reveal that the Ni-ferrierite sample oxidized by dioxygen provides the best performance in the direct oxidation of methane to methanol. It should be noted that possible subsequent oxidation steps in the methane transformation to the other oxidized products may lead to lower methanol yields (see the ESI,† Fig. S4). Moreover, interactions of methanol and other oxidation products of

Table 1 The concentrations of bare cations and the cations in the β cationic site calculated from FTIR results and CH_3OH yields estimated from mass spectrometry experiments

	Ni-FER	Mn-FER	Co-FER
M(II)$_{bare}$ [mmol g^{-1}]	0.17	0.35	0.25
M(II)$_β$ [mmol g^{-1}]	0.10	0.16	0.16
Yield of CH_3OH [μmol g$^{-1}_{cat}$]	116	42	20
CH_3OH/M(II)$_{bare}$ [mol mol^{-1}]	0.68	0.12	0.08
CH_3OH/M(II)$_β$ [mol mol^{-1}]	1.16	0.26	0.13

methane oxidation with the adsorption centers in the ferrierite matrix (*e.g.*, M(II) cations in the other cationic sites, Brønsted protonic sites (Al–OH–Si), and terminal silanol groups (Si–OH)) cannot be excluded. Therefore, the yields in Table 1 evidence the activity of the M-ferrierite (M = Ni, Mn, and Co) samples in the cleavage of dioxygen and the subsequent selective oxidation of methane but do not reflect quantitatively their ability of splitting dioxygen.

In summary, our experimental data confirmed that the distant binuclear transition metal (M = Ni, Mn, Co) cationic centers stabilized in the ferrierite matrix perform splitting of dioxygen already at RT into a pair of α-oxygen atoms. The presence of the methanol in the methane stream after interaction of methane and dioxygen oxidized M-ferrierite already at RT, undoubtedly evidenced engagement of α-oxygen in methane oxidation. In contrast to other zeolitic systems, methanol produced over the distant binuclear cationic structures can be released to the gas phase from the M-ferrierite samples without the usage of an effluent, proving previous protonation of the methoxy species.

The selective oxidation of methane to methanol by dioxygen evidences that the distant binuclear cationic structures in M-ferrierites (M = Ni, Mn, and Co) exhibit a general ability to undergo an M(II) → M(IV) redox cycle and thus split dioxygen to form a pair of α-oxygens. Until now, the ability to cleave dioxygen and directly oxidize methane to methanol has been reported exclusively for Fe-ferrierite. This study presents new systems featuring stable distant binuclear transition metal centers (Ni, Mn, Co), that are robust and easy for preparation up to high concentrations. The presented results can serve as a base for the development of materials and technology for the utilization of natural gas *via* the selective oxidation of methane by dioxygen.

Conflicts of interest

There are no conflicts to declare.

Notes and references

1 K. T. Dinh, M. M. Sullivan, P. Serna, R. J. Meyer, M. Dinca and Y. Roman-Leshkov, *ACS Catal.*, 2018, **8**, 8306–8313.
2 K. Narsimhan, K. Iyoki, K. Dinh and Y. Román-Leshkov, *ACS Cent. Sci.*, 2016, **2**, 424–429.
3 B. E. R. Snyder, P. Vanelderen, M. L. Bols, S. D. Hallaert, L. H. Bottger, L. Ungur, K. Pierloot, R. A. Schoonheydt, B. F. Sels and E. I. Solomon, *Nature*, 2016, **536**, 317–321.
4 E. Tabor, J. Dedecek, K. Mlekodaj, Z. Sobalik, P. C. Andrikopoulos and S. Sklenak, *Sci. Adv.*, 2020, **6**, eaaz9776.
5 J. Xu, Q. Wang and F. Deng, *Acc. Chem. Res.*, 2019, **52**, 2179–2189.
6 B. E. R. Snyder, M. L. Bols, R. A. Schoonheydt, B. F. Sels and E. I. Solomon, *Chem. Rev.*, 2018, **118**, 2718–2768.
7 A. J. Knorpp, M. A. Newton, S. C. M. Mizuno, J. Zhu, H. Mebrate, A. B. Pinar and J. A. van Bokhoven, *Chem. Commun.*, 2019, **55**, 11794–11797.
8 M. A. Newton, A. J. Knorpp, V. L. Sushkevich, D. Palagin and J. A. van Bokhoven, *Chem. Soc. Rev.*, 2020, **49**, 1449–1486.
9 V. L. Sushkevich and J. A. van Bokhoven, *Catal. Sci. Technol.*, 2020, **10**, 382–390.
10 V. L. Sushkevich, R. Verel and J. A. van Bokhoven, *Angew. Chem., Int. Ed.*, 2020, **2**, 910–918.
11 D. Palagin, V. L. Sushkevich and J. A. van Bokhoven, *ACS Catal.*, 2019, **9**, 10365–10374.
12 J. H. Lee, W. Bonte, S. Corthals, F. Krumeich, M. Ruitenbeek and J. A. van Bokhoven, *Ind. Eng. Chem.*, 2019, **58**, 5140–5145.
13 M. Ravi, M. Ranocchiari and J. A. van Bokhoven, *Angew. Chem., Int. Ed.*, 2017, **56**, 16464–16483.
14 K. Jisa, J. Novakova, M. Schwarze, A. Vondrova, S. Sklenak and Z. Sobalik, *J. Catal.*, 2009, **262**, 27–34.
15 S. Sklenak, P. C. Andrikopoulos, B. Boekfa, B. Jansang, J. Novakova, L. Benco, T. Bucko, J. Hafner, J. Dedecek and Z. Sobalik, *J. Catal.*, 2010, **272**, 262–274.
16 E. Tabor, M. Lemishka, Z. Sobalik, K. Mlekodaj, P. C. Andrikopoulos, J. Dedecek and S. Sklenak, *Commun. Chem.*, 2019, **2**, 71.
17 M. Lemishka, J. Dedecek, K. Mlekodaj, Z. Sobalik, S. Sklenak and E. Tabor, *Pure Appl. Chem.*, 2019, **91**, 1721–1732.
18 J. Dedecek, E. Tabor, P. C. Andrikopoulos and S. Sklenak, *Int. J. Quantum Chem.*, 2021, **121**, e26611.
19 G. Sadovska, E. Tabor, P. Sazama, M. Lhotka, M. Bernauer and Z. Sobalik, *Catal. Commun.*, 2017, **89**, 133–137.
20 E. Tabor, G. Sádovská, M. Bernauer, P. Sazama, J. Nováková, V. Fíla, T. Kmječ, J. Kohout, K. Závěta and Z. Sobalík, *Appl. Catal., B*, 2019, **240**, 358–366.
21 J. Dedecek, E. Tabor and S. Sklenak, *ChemSusChem*, 2019, **12**, 556–576.
22 J. Dedecek, M. J. Lucero, C. B. Li, F. Gao, P. Klein, M. Urbanova, Z. Tvaruzkova, P. Sazama and S. Sklenak, *J. Phys. Chem. C*, 2011, **115**, 11056–11064.